INTERNATIONAL JOURNAL FOR NUMERICAL METHODS IN FLUIDS
Int. J. Numer. Meth. Fluids 2002; **38**:945–962 (DOI: 10.1002/fld.242)

Asymmetric flows in planar symmetric channels with large expansion ratio

Sanjay Mishra and K. Jayaraman[†,*]

Department of Chemical Engineering, Michigan State University, East Lansing, MI 48824, U.S.A.

SUMMARY

A continuation method has been used with a finite element grid and a geometric perturbation to compute two successive symmetry breaking flow transitions with increasing Reynolds number in flow of generalized Newtonian fluids through a sudden planar expansion. With an expansion ratio of 16, the onset Reynolds number is particularly sensitive to small geometric asymmetry and the critical Reynolds numbers for the two successive flow transitions are found to be very close. These transitions are delayed to higher onset Reynolds numbers by increasing the degree of pseudoplasticity. This trend is observed experimentally as well in this work and may be attributed to the competing effects of shear thinning and inertia on the size of the corner vortex before the symmetry breaking flow transition. After the second transition with an expansion ratio of 16, the two large staggered vortices on opposite walls occupy most of the transverse dimension so that the core flow between the vortices appears as a thin jet oscillating along the flow direction. This is more pronounced for the pseudoplastic liquid. After the second transition, the degree of flow asymmetry at a given location downstream of the expansion plane is larger for the pseudoplastic liquid than for the Newtonian liquid at comparable Reynolds numbers. The last feature is also evident in the experimentally observed velocity profiles. Copyright © 2002 John Wiley & Sons, Ltd.

KEY WORDS: asymmetric flow; sudden expansion; instability, bifurcation, transition

1. INTRODUCTION

The onset of asymmetric flow patterns in laminar, incompressible flow of Newtonian fluids above a critical Reynolds number through a sudden, planar symmetric expansion is well documented [1–8] in terms of experimental observations as well as computations. The geometry and notation are laid out in Figure 1; the expansion ratio β refers to the ratio of downstream channel height H to the upstream channel height h, while the aspect ratio refers to the ratio of channel width to channel height in the downstream section. The Reynolds number is based on the mean inlet velocity U_{av} and the half height of the upstream channel:

$$Re = (h/2)\rho U_{av}/\mu \tag{1}$$

*Correspondence to: K. Jayaraman, Department of Chemical Engineering, Michigan State University, 2527 Engineering Building, East Lansing, MI 48824, U.S.A.
[†]E-mail: jayarama@egr.msu.edu

Received July 2000
Revised April 2001

Copyright © 2002 John Wiley & Sons, Ltd.

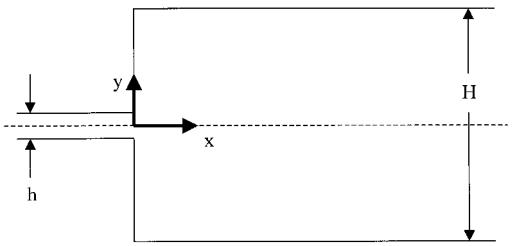

Figure 1. Schematic of a plane sudden expansion.

where ρ and μ denote the density and viscosity of the fluid respectively. For comparison with other work, it is noted that the mean inlet velocity is 2/3 of the maximum inlet velocity for plane Poiseuille flow. The critical Reynolds number is not very large and decreases with increasing expansion ratio and with increasing aspect ratio of the channel. For example, Cherdron *et al.* [1] have observed that with a channel aspect ratio downstream of 8, the critical Reynolds number (as defined above) drops from 62 for a 1:2 expansion to about 27 for a 1:3 expansion.

The flow remains steady and two-dimensional after the onset of asymmetry. Right after the onset, the asymmetric flow is associated with a larger corner vortex adjacent to one of the walls; at higher *Re*, three vortices appear with two along one wall and one along the other wall. The results of analysis by Alleborn *et al.* [4] and by Shapira *et al.* [6] confirm that the asymmetric steady states are stable and that the flow bifurcates from a stable symmetric steady state solution to two stable, asymmetric steady state solutions with the larger vortex near either wall. Increasing the Reynolds number beyond the critical value leads to progressively more asymmetric flow patterns as observed by Cherdron *et al.* [1] with laser Doppler anemometry in a 1:2 expansion. Thus, the flow bifurcation is supercritical. Furthermore, the asymmetry persisted over greater flow lengths as well. For example, at Reynolds numbers just above the critical value, the symmetry of the velocity profile was restored at a downstream location $x/H = 16$; but at a Reynolds number of twice the critical value – still before any further flow transition, the asymmetry persisted over greater flow lengths. At higher Reynolds numbers, a second transition leading to three vortices in a two-dimensional, steady velocity field has been reported by Durst *et al.* [3], Fearn *et al.* [5], etc. After the second flow transition, the positioning of the three vortices and their sizes along both the flow direction and the transverse direction, lead to a core flow that oscillates to different extents. The multiplicity of steady state solutions with Newtonian fluids is a consequence of the nonlinearity of the equations of motion at nonzero Reynolds numbers. The present paper explores the effect of fluid nonlinearity on the asymmetric flow patterns obtained in a symmetric, planar expansion, with both computations and experiment.

Computations of asymmetric flow fields in Newtonian fluids flowing through a planar expansion with a single inlet have been carried out with a variety of perturbations [3–8] from the basic symmetric two-dimensional steady state. Durst and coworkers [3, 4] perturbed the inlet velocity profile. Fearn *et al.* [5] investigated the effect of perturbations in the geometry of the channel and concluded that a small vertical shift of the downstream grid with respect to the inlet led to predictions of a continuous rise in flow asymmetry with increasing Reynolds number. Shapira *et al.* [6] point out that in order to obtain an asymmetric solution, it was

Copyright © 2002 John Wiley & Sons, Ltd.

necessary to start with an asymmetric initial flow field. Their linear stability analysis also confirmed that the symmetric solution loses stability above a critical Reynolds number that corresponded to the bifurcation point. Teschauer [7] introduced slight asymmetry in the upstream channel to compute the bifurcated branch of the solution for expansion ratios ranging from 1.5 to 3. The results of Shapira *et al*. [6] and Teschauer [7] have recently been confirmed by the work of Drikakis [8]. Drikakis has computed bifurcation curves with several numerical schemes based on a finite volume approach for expansion ratios up to 6 and predicted critical Reynolds numbers of 72 and 27 respectively for expansion ratios of 2 and 3.

Other researchers [9, 10] have carried out computations on expansions with multiple inlets and predicted a wide variety of flow transitions. Foumeny *et al.* [9] employed the CFD code FLUENT to predict the degree of flow asymmetry successfully for a single inlet channel with a 1:3 expansion and then predicted that the transition to asymmetric flows occurs at lower Reynolds numbers in multiple inlet channels. Above this critical value, the degree of asymmetry increases gradually over a much larger range of Reynolds numbers than in the case of the single inlet channel. Goodwin and Schowalter [10] used a continuation approach coupled with an asymmetric perturbation of the flow rates in the two inlets. The flow fields at the lower Reynolds numbers were used as initial iterates for computations at higher Reynolds numbers. At sufficiently high Reynolds numbers, the flow was re-balanced between the two inlets and the same continuation approach was used with progressively decreasing Reynolds numbers.

The object of the present paper is to examine the details of the asymmetric flow patterns obtained in steady flow of incompressible shear thinning fluids through planar expansions. This is done with a large expansion ratio of 16 because the flow transitions occur at particularly low Reynolds numbers with large expansion ratios. A continuation procedure that is started with a geometric perturbation has been used to compute the asymmetric velocity fields. Experimental measurements of the velocity fields in a 1:16 expansion were obtained by laser Doppler velocimetry with Newtonian and non-Newtonian model fluids.

2. GOVERNING EQUATIONS

Steady, two-dimensional, isothermal flow of an incompressible, power law fluid through an abrupt planar expansion (see Figure 1) without gravity in the plane of flow is described by the following equations

$$\frac{\partial U_x}{\partial x} + \frac{\partial U_y}{\partial y} = 0 \tag{2}$$

$$\rho\left(U_x\frac{\partial U_x}{\partial x} + U_y\frac{\partial U_x}{\partial y}\right) = -\frac{\partial p}{\partial x} + \frac{\partial \tau_{xx}}{\partial x} + \frac{\partial \tau_{yx}}{\partial y} \tag{3}$$

$$\rho\left(U_x\frac{\partial U_y}{\partial x} + U_y\frac{\partial U_y}{\partial y}\right) = -\frac{\partial p}{\partial y} + \frac{\partial \tau_{xy}}{\partial x} + \frac{\partial \tau_{yy}}{\partial y} \tag{4}$$

$$\underline{\underline{\tau}} = K(II_\gamma)^{n-1}\underline{\underline{\dot{\gamma}}} \tag{5}$$

where U_x and U_y are the axial and transverse components of velocity, $\underline{\underline{\tau}}$ is the deviatoric stress tensor, $\underline{\underline{\dot{\gamma}}}$ is the strain rate tensor, II_γ is the second invariant of the strain rate tensor, p is the

Copyright © 2002 John Wiley & Sons, Ltd.

pressure and ρ is the fluid density. The velocities are scaled with the maximum velocity in the inlet channel while x is scaled with the upstream channel height h and y is scaled with the half height of the larger channel.

$$U = \frac{U_x}{U_{\max}}; \quad V = \frac{U_y}{U_{\max}}; \quad X = \frac{x}{h}; \quad Y = \frac{y}{H/2} \tag{6}$$

The domain of the problem is $-l_1 < X < l_2$ and $-1 < Y < 1$. l_1 and l_2 were taken to be 5 and 65 step heights respectively. The step height in dimensionless terms is $(\beta - 1)/\beta$. Reducing the values of l_1 and l_2 by 50 per cent changed the solution only by 0.01 per cent. The boundary conditions written in terms of these scaled variables are as follows

$$U\left(X, \pm\frac{1}{\beta}\right) = V\left(X, \pm\frac{1}{\beta}\right) = 0 \quad \text{for} \quad -l_1 < X < 0 \tag{7}$$

$$U(0, Y) = 0 \quad \text{for} \quad \pm\frac{1}{\beta} \leqslant Y \leqslant +1 \tag{8}$$

$$U(X, \pm 1) = V(X, \pm 1) = 0 \quad \text{for} \quad 0 < X < l_2 \tag{9}$$

$$U(-l_1, Y) = 1 - Y^{1+1/n}; \quad V(-l_1, Y) = 0 \tag{10}$$

The Reynolds number Re^* is redefined for the power law fluid as follows

$$Re^* = \frac{(h/2)^n U_{av}^{2-n} \rho}{K[(2 + 1/n)]^{n-1}} \tag{11}$$

3. NUMERICAL SCHEME

These equations were solved by finite element calculations with a CFD code FIDAP (Fluent, Inc.). A continuation method coupled with an initial geometric perturbation was used to solve for the asymmetric flow fields. The mesh was graded finely in all the corners and was less dense away from the corners. Figure 2 shows the variation of the grid density in the channel. In the axial direction (i.e., along the X axis), the mesh density was greatest close to the $X = 0$ plane. In the transverse direction, the mesh was more dense near both the 90° corners ($Y = \pm 1$) and the 270° corners ($Y = \pm 1/\beta$) and was less dense in between. Nine node, isoparametric quadrilateral elements were used in the computations. The velocity field was represented in terms of bi-quadratic interpolating functions while the pressure was represented in terms of linear shape functions. The Newton–Raphson method was used to solve the algebraic equations for nodal values. The iteration was terminated when the following tolerances were met by the velocity change between iterations and the residual, with the root mean square norm

$$\|V_i - V_{i-1}\|/\|V_{i-1}\| < 10^{-6}, \quad \|R_i\|/\|R_{i-1}\| < 10^{-6} \tag{12}$$

The perturbation–continuation method used in this work is described in Figure 3. Figure 3(a) describes the domain perturbation while Figure 3(b) illustrates the progress of the coupled

Copyright © 2002 John Wiley & Sons, Ltd.

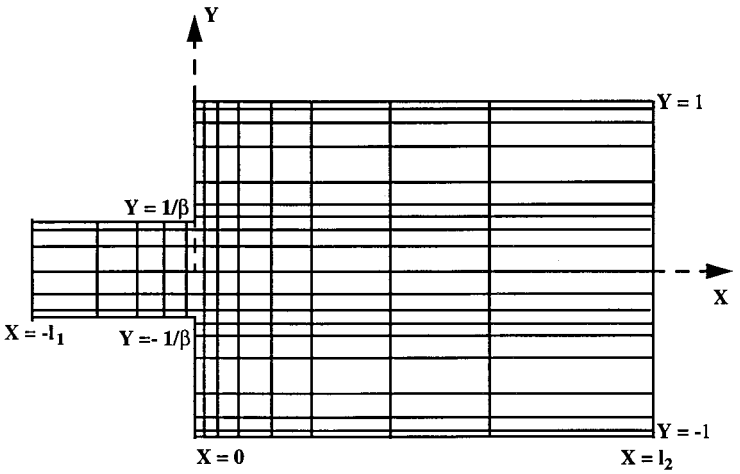

Figure 2. Illustration of graded mesh used for calculations.

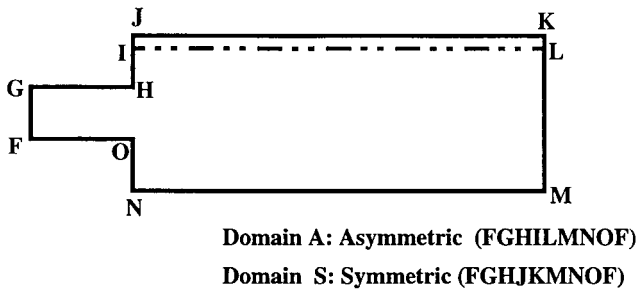

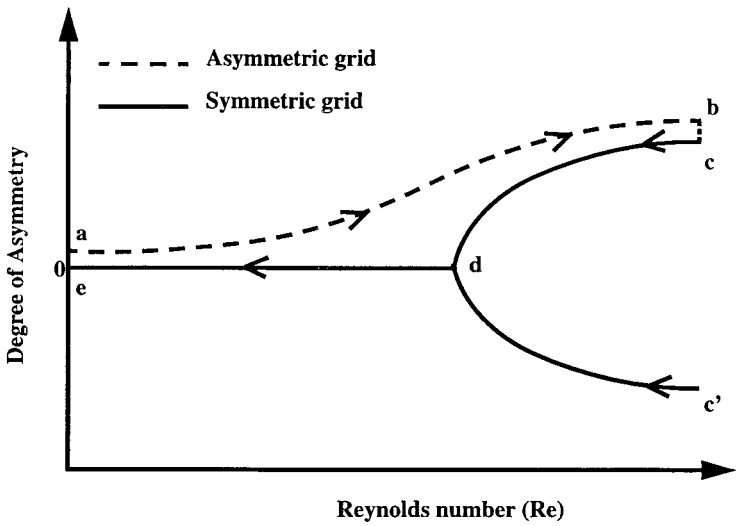

Figure 3. The continuation approach with an initial geometric perturbation.

Copyright © 2002 John Wiley & Sons, Ltd.

perturbation–continuation method. An asymmetric perturbation is introduced in the geometry of the configuration by shortening one of the steps from JH to IH. This resulted in IH being about 2 to 5 per cent shorter than the step ON. The Stokes solution was then computed for this asymmetric channel. Using the Stokes solution as the initial iterate for the next run, the equations of motion were solved for a higher Reynolds number. For every subsequent *Re*, the result of the previous computation was used as the initial guess. This procedure was continued until point b, where the degree of asymmetry in the flow is much greater than that in the geometry. At this point, the computational grid was made symmetric and the solution was then computed for the symmetric domain S using the results at point b for domain A as the initial iterate. Subsequently the continuation method was repeated on the symmetrical grid with the Reynolds number now being reduced gradually from point c to e. At point d, the bifurcation point (or the critical Reynolds number) was crossed over, below which the flow was essentially symmetric. The increment in *Re* ranged from 0.25 to 2, depending on the expansion ratio being considered. The final solution for the symmetric channel was independent of the extent of initial grid perturbation as discussed in the sections on results. When the continuation is carried out to higher Reynolds numbers than at c or c′ on a symmetric grid, a second flow transition is obtained.

4. RESULTS AND DISCUSSION

Validation of the perturbation–continuation approach

The accuracy of the continuous-perturbation approach is demonstrated by comparing our results with existing computational results for Newtonian flow through a 1:3 planar expansion. The degree of asymmetry in the flow is represented on bifurcation diagrams here by the difference in the reattachment lengths on the two walls, normalized by the step height. Other measures that could have been used are the difference in the wall shear stresses, the centerline normal velocity component or the shear rate in the center of the channel. The reattachment lengths were evaluated as follows: the sign of the axial velocity was monitored along the nodal layer closest to the walls and two successive nodes with negative and positive u-velocity were identified. A simple linear interpolation then yielded the reattachment length, which is denoted by L_v after dividing by the step height. Figure 4 demonstrates the three branches of the bifurcation curve resulting from the perturbation–continuation approach for a symmetric channel with expansion ratio of 3. Up to $Re = 27$, the symmetric solution is the only steady state (i.e. the difference in the reattachment lengths is zero); this is consistent with experiments. At *Re* greater than 27, the vortex lengths become unequal. The degree of asymmetry increases with increasing Reynolds number. Either of the asymmetric steady states represented by branches 2 and 3 may be followed at $Re > 27$. Figure 4 also reveals that a small degree of asymmetry in the geometry hastens the flow transition considerably changing the critical Reynolds number to less than 20. The onset Reynolds number of 27 for Newtonian flow through a 1:3 planar expansion predicted with the perturbation–continuation approach of this work is in very close agreement with the computed results of Fearn *et al.* [5]. It might be noted here that the Reynolds number defined by Drikakis [8] is three times the Reynolds number defined here. In the following sections we present new results for a 1:16 expansion describing the effect of shear thinning on the asymmetric flow patterns.

Copyright © 2002 John Wiley & Sons, Ltd.

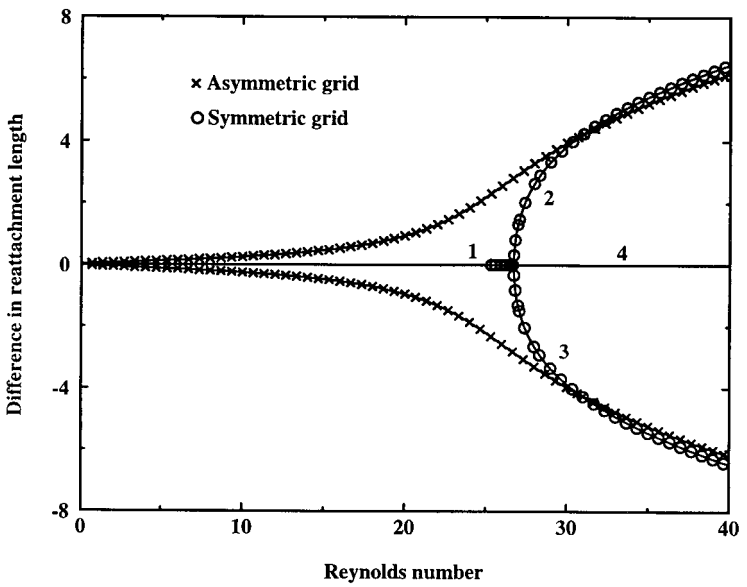

Figure 4. Demonstration of the perturbation–continuation approach for Newtonian flow through a 1:3 planar expansion.

Predicted flow transitions in a 1:16 expansion

Computations for the 1:16 channel are more taxing because of the more severe corner singularity and the denser mesh grading required close to the corners. The effect of grid resolution on the outcome of our calculations was investigated for the expansion ratio of 16 with two different grids – G2 and G3 having 5871 and 11431 nodes respectively. The bifurcation diagram for a Newtonian liquid in the 1:16 expansion is presented in Figure 5 along with a comparison of the performance of grids G2 and G3. The results from G2 and G3 were nearly identical. Our computations for a Newtonian liquid flowing through a 1:16 planar channel predict a critical Reynolds number of 6.3.

Computations for shear thinning liquids were carried out with parameters given in Table I. Here η is the shear viscosity, $\dot{\gamma}$ is the shear rate and k and n are rheological constants called the consistency index and the shear-thinning index respectively. The critical Re^* for $n=0.7$ in a 1:16 channel was computed to be 18.5. Shear thinning, therefore, delayed the onset of asymmetry. The bifurcation curve for $n=0.7$ is shown in Figure 6. The flow field is symmetric up to a critical Re^* of 18.5. As the Reynolds number is increased above this critical value, the difference in reattachment lengths increases to around 3 at $Re^*=35$. With a greater extent of shear thinning ($n=0.5$), bifurcation was predicted at an even higher Reynolds number of around 27.5, as shown on Figure 7. This arises from the competing effects of shear thinning and inertia on the size of the corner vortex before the symmetry breaking flow transition. While the reattachment length in a 1:16 expansion computed here and checked with experiment for a Newtonian liquid follows the relation $L_v=0.425+0.18Re$, the corresponding relation checked with experiment for the P1 solution is found to be $L_v=0.22+0.07Re^*$. In the case of shear thinning fluids, the slower fluid in the corner vortex has a higher viscosity than the fluid

Copyright © 2002 John Wiley & Sons, Ltd.

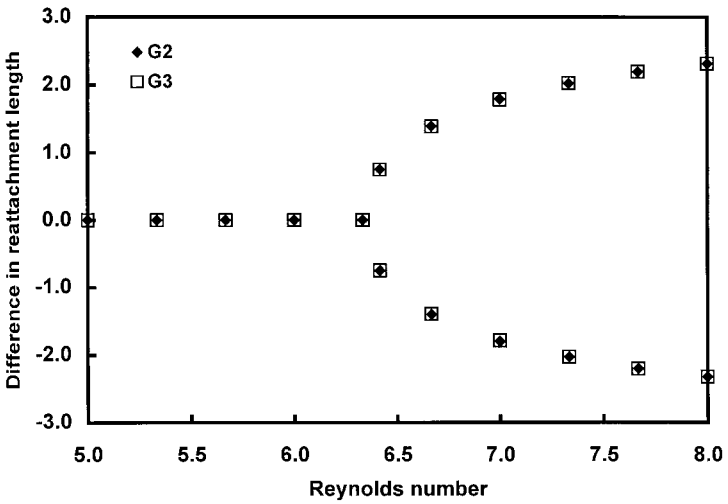

Figure 5. Bifurcation curve for Newtonian flow in a 1:16 expansion with the results of mesh refinement.

Table I. Parameters used in the viscosity model.

Designation	n	$K\ (Pa-s^n)$
P1	0.7	7.82
P2	0.5	77.46

outside the vortex and this leads to smaller corner vortices for the same Reynolds number than with Newtonian fluids—cf. Giaquinta and Hung [11]. This competition between inertia and shear thinning leads to a higher onset Reynolds number for flow asymmetry in abrupt planar expansions.

It is instructive to examine the sensitivity of the asymmetry in the flow pattern to small amounts of geometrical asymmetry in the 1:16 expansion. Grid asymmetry is defined by the expression $100(\Delta H)/(H/2)$ where H is the total gap height of the larger channel and ΔH is the reduction in the step height on one side. This parameter has been varied from 0 to 3.1 per cent to obtain the bifurcation curves presented in Figure 8 for a Newtonian fluid and in Figure 9 for a shear thinning fluid with $n=0.7$. Only the positive branch of the bifurcation curve is shown in these figures for clarity. The departure of the asymmetric grid curves from the result for symmetric expansions is noticeable for the Newtonian fluid at a Reynolds number of 4 compared to the critical Reynolds number of 6.3 for the symmetric geometry. This departure is evident in Figure 9 too at Reynolds numbers much lower than the critical Reynolds number for the symmetric geometry. These figures show that the departure of the curves from the result for symmetric expansions is significant for a small amount of geometric asymmetry with both fluids and is more pronounced with the shear thinning fluid.

Copyright © 2002 John Wiley & Sons, Ltd.

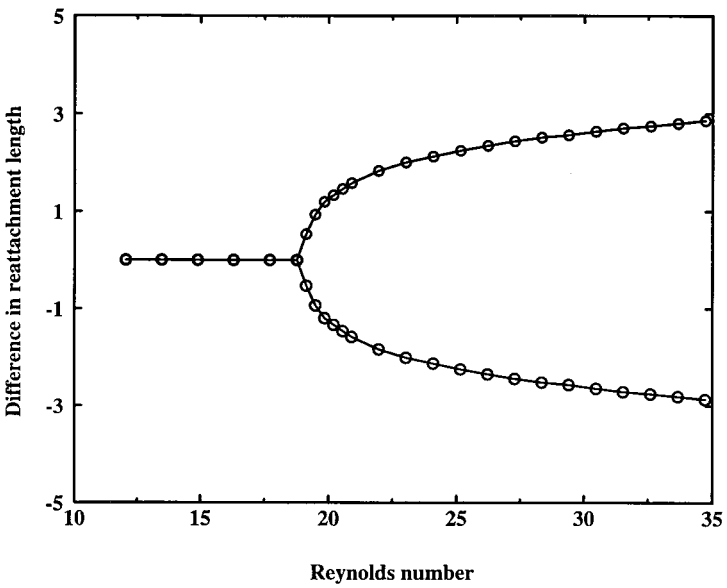

Figure 6. Bifurcation curve for the shear thinning liquid P1 ($n = 0.7$) in a 1:16 expansion.

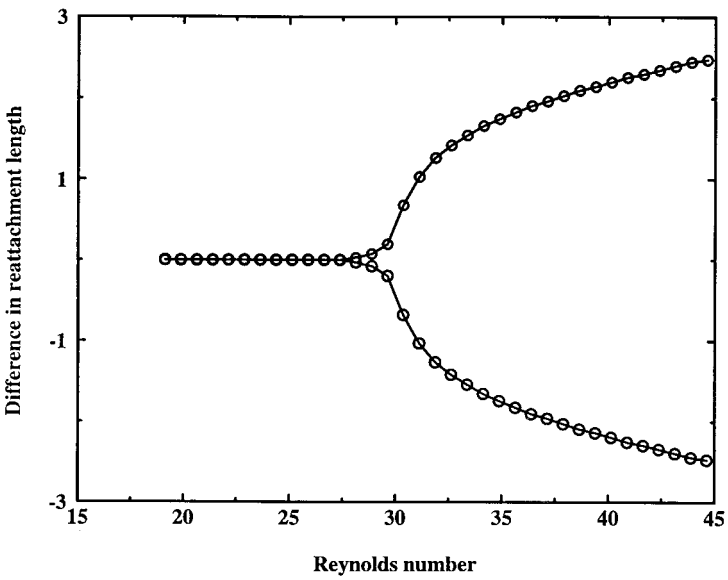

Figure 7. Bifurcation curve for a shear thinning liquid with $n = 0.5$ in a 1:16 expansion.

The streamlines showing the effect of increasing Reynolds numbers on the flow patterns for a Newtonian fluid in a 1:16 expansion are shown in Figure 10(a) through (d). The corner vortices for the large expansion ratios fill up most of the transverse length of the downstream

Copyright © 2002 John Wiley & Sons, Ltd.

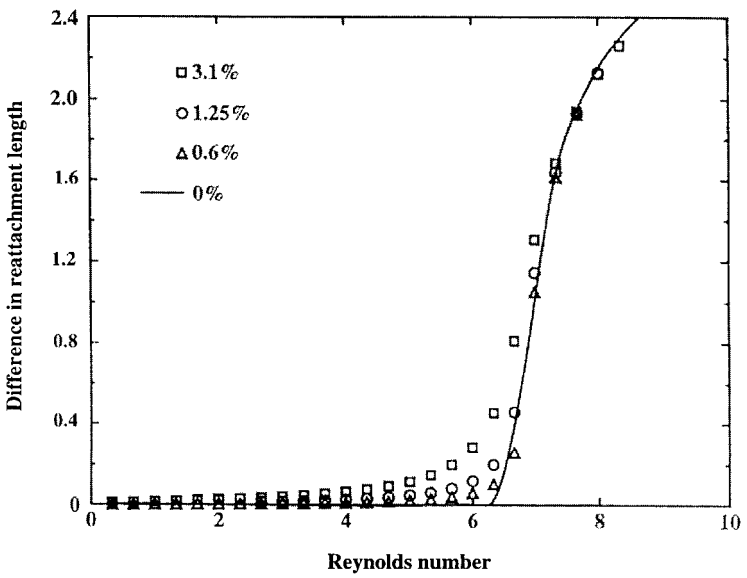

Figure 8. Effect of geometrical asymmetry on Newtonian flow bifurcation in a 1:16 expansion.

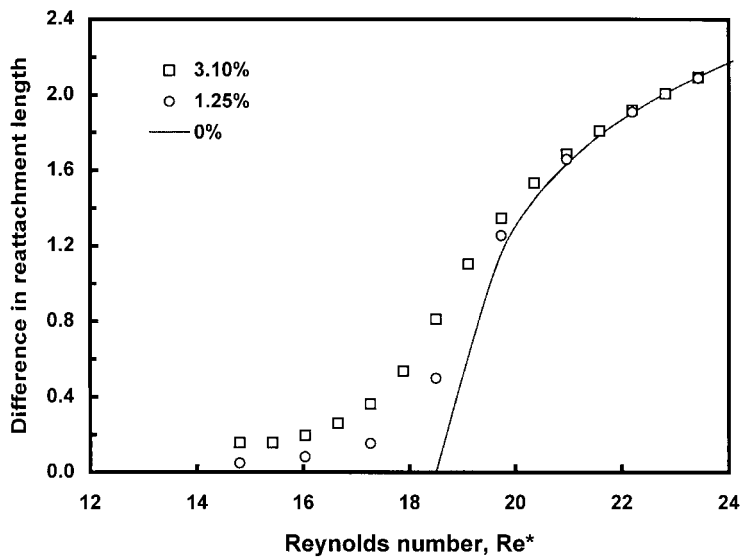

Figure 9. Effect of geometrical asymmetry on pseudoplastic flow bifurcation in a 1:16 expansion ($n = 0.7$).

channel close to the expansion plane, resulting in a thinner core between the recirculation zones. The second flow transition resulting in three vortices was detected at around $Re = 13$. The two large vortices are staggered on opposite walls as shown in Figure 10(d); either one

Copyright © 2002 John Wiley & Sons, Ltd.

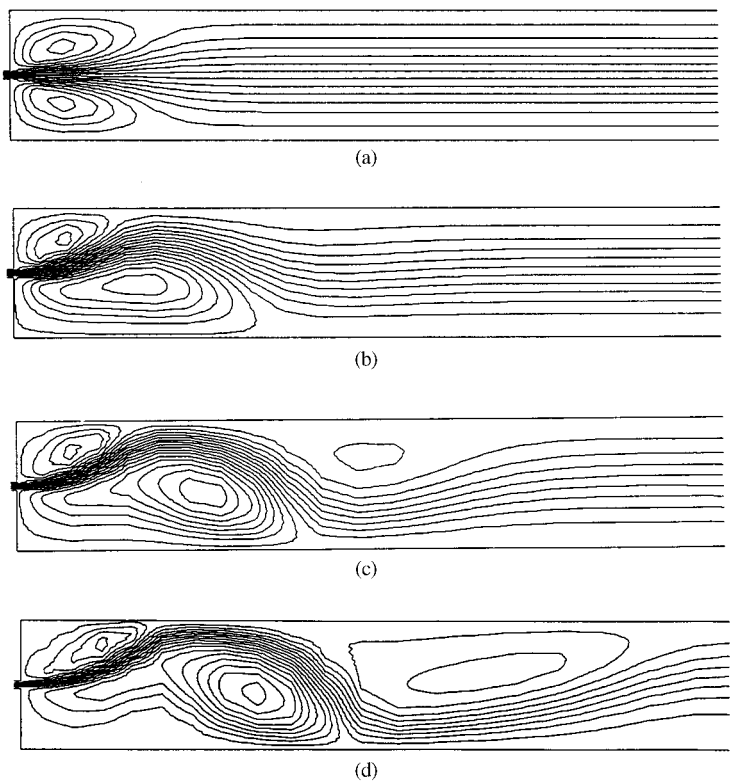

Figure 10. Computed flow patterns at different Reynolds numbers for a Newtonian liquid in a 1:16 expansion. (a) $Re = 6$ (b) $Re = 8$ (c) $Re = 14$ and (d) $Re = 24$.

of these vortices occupies most of the gap exacerbating the spatial oscillation of the core flow. The two distinct transitions appear at a much closer Re interval than in channels with a smaller expansion ratio. This trend is consistent with the results of stability calculations by Alleborn *et al.* [4] for an expansion ratio of 1000.

The types of flow transitions predicted for the shear thinning liquid are similar to the ones predicted for the Newtonian liquid. Figures 11(a) through (d) depict the flow patterns for a shear thinning solution (P1) flowing through the 1:16 expansion. At $Re^* = 18$, the two corner vortices are of equal lengths. Figure 11(b) shows that at $Re^* = 20$, the reattachment lengths are unequal and the difference in the reattachment length increases at higher Reynolds numbers (seen in Figure 11(c)). Once again, the vortices in high expansion ratio channels grow in the transverse direction, making the core flow meander significantly. At high Reynolds numbers, a thin jet of liquid in the core is seen to move toward one wall and then toward the other. At around $Re^* = 44$, the second flow transition is detected, wherein three vortices coexist in the channel. The larger vortex in Figure 11(d) at the onset of the second transition is considerably larger than the corresponding vortex for the Newtonian liquid in Figure 10(c).

Copyright © 2002 John Wiley & Sons, Ltd.

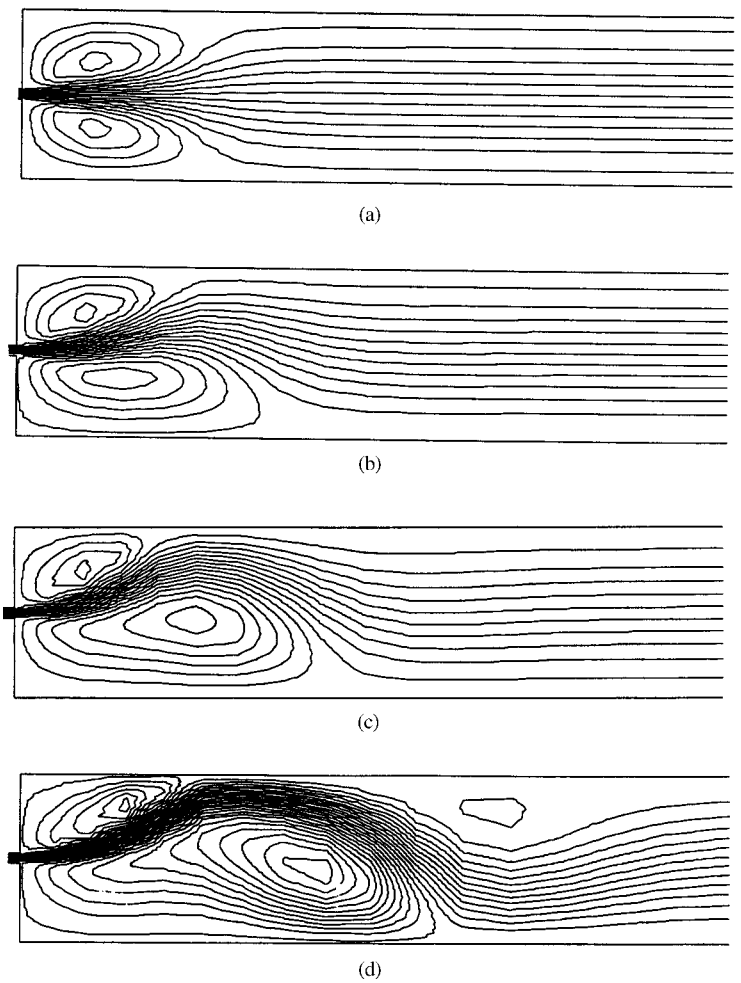

Figure 11. Computed flow patterns at different Reynolds numbers with the shear thinning liquid P1 in a 1:16 channel. (a) $Re^* = 18$ (b) $Re^* = 20$ (c) $Re^* = 25$ and (d) $Re^* = 44$.

The spatial oscillation of the core jet can be seen from a comparison of velocity profiles computed after the onset of the asymmetry. The velocity profiles computed for different axial locations at $Re = 25.3$ for a Newtonian liquid in a 1:16 expansion are presented in Figure 12. These velocity profiles correspond to the streamlines shown in Figure 10(d) ($Re = 24$). At $X = 5$, two recirculation regions corresponding to the two corner vortices are seen. At the other two axial locations, $X = 30$, and $X = 60$, only one recirculation region is detected – but near opposite walls. At $X = 5$, the positive peak of the velocity is offset by only 0.05 units along the y-coordinate. At $X = 30$, the peak is offset by 0.6 units on the same side of the centerline. But at $X = 60$, the peak is offset by -0.6 units – appearing on the other side of the centerline. The peak velocity itself is attenuated with distance as expected, with restoration

Copyright © 2002 John Wiley & Sons, Ltd.

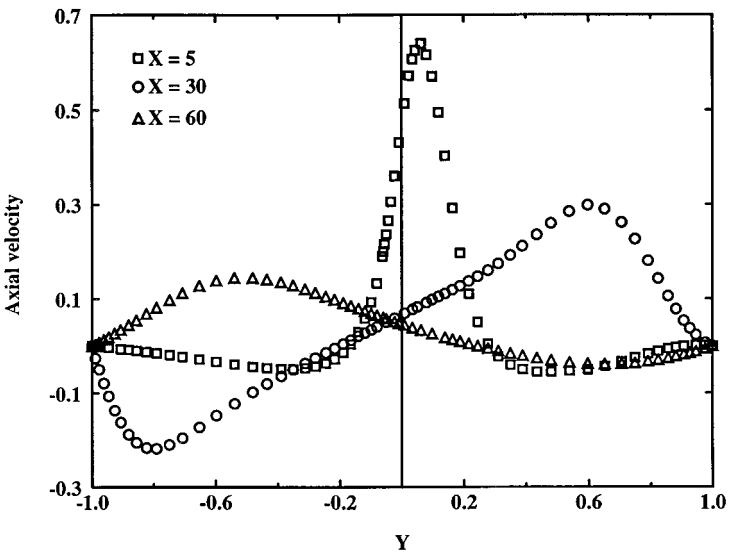

Figure 12. Computed velocity profiles with a Newtonian liquid at different axial locations in a 1:16 expansion for $Re = 25.3$.

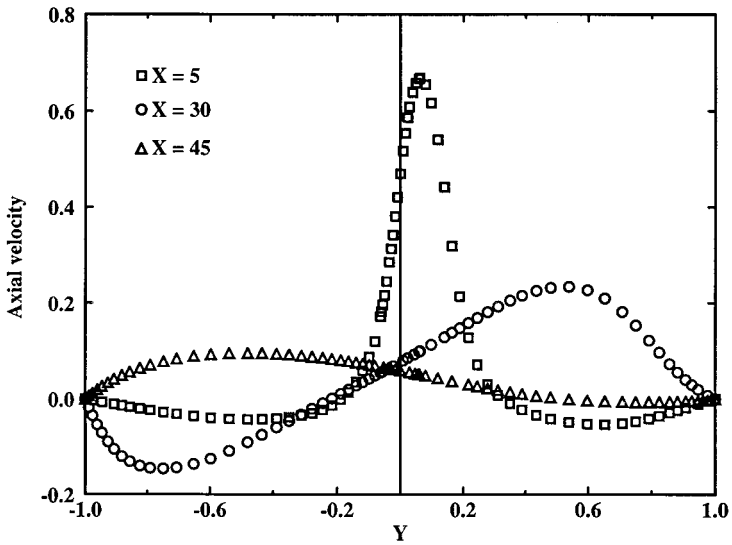

Figure 13. Computed velocity profiles of the shear thinning liquid P1 at $Re^* = 44.3$.

of symmetry far downstream. The velocity profiles for the shear thinning liquid ($n = 0.7$) at different axial locations with $Re^* = 44.3$ after the onset of the second flow transition, are presented in Figure 13 (also see Figure 11(d)). In this set, two recirculation regions are

Copyright © 2002 John Wiley & Sons, Ltd.

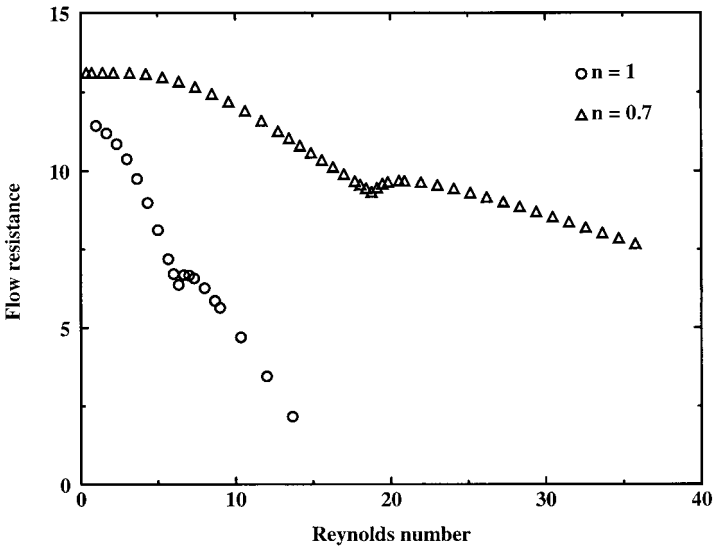

Figure 14. (fRe) vs Reynolds number for two different liquids ($n=1$ and $n=0.7$): Note the increase after a break at the critical Reynolds number.

present at $X=5$ and one at $X=30$, but at $X=45$, there is no recirculating region. This is consistent with the third vortex being much smaller in Figure 11(d) for the shear thinning liquid. At $X=5$, the velocity peaks at around $Y=0.05$. Further downstream at $X=30$ and 45, the velocity peaks at $Y=0.5$ and -0.5 units respectively, on opposite sides.

Pressure drop and flow resistance

The pressure drop in the upstream and downstream sections to and from the plane of expansion may be combined into a flow resistance as follows

$$f\,Re = 2Re\left[\frac{H((-\Delta P)/\rho U_{av}^2)_d + h((-\Delta P)/\rho U_{av}^2)_u}{l_1 + l_2}\right]$$

This quantity has been evaluated for the Newtonian liquid and the shear thinning liquid with $n=0.7$ through a 1:16 expansion and plotted in Figure 14. A break is seen after the corresponding onset Reynolds number on either curve, where the flow resistance goes up before starting another decline. The curve of fRe for the shear thinning liquid is higher because the extent of pressure recovery is lower for the shear thinning liquid.

Experimental

A transparent flow cell was constructed with inserts placed in a gap between two large plates such that the upstream gap $h=2.54$ mm (or 0.1 in.) and the downstream gap $H=40.6$ mm (or 1.6 in.). The channel was 16 in. wide both upstream and downstream so that the aspect ratio of the downstream channel was 10. The total length of the plane channel was 15 in. with the plane of expansion at 6 in. from the inlet as shown in Figure 15. Two rectangular

Copyright © 2002 John Wiley & Sons, Ltd.

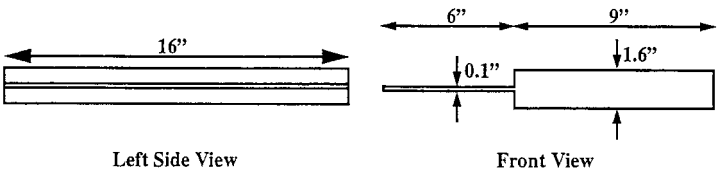

Figure 15. Test channel: schematic and dimensions.

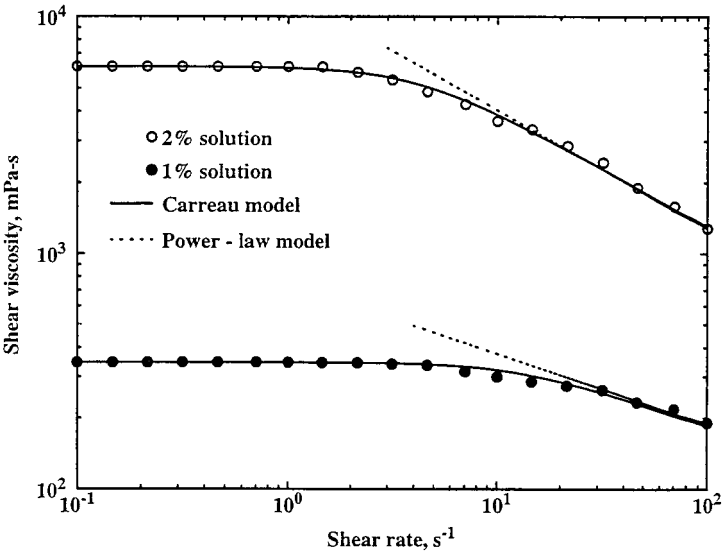

Figure 16. Shear viscosity curves of two shear thinning liquids P1 and P2.

inserts of 19.05 mm (or 0.75 in.) thickness were used to provide an upstream gap of 2.54 mm (or 0.1 in.). The inserted plates were specially ordered Plexiglass sections with less than 1 per cent variation in their thickness. This could lead to variations of up to 10 per cent in the upstream channel gap; the actual variation in the expansion ratio was under 5 per cent.

Velocity profiles before and after the flow transition were obtained in the downstream section of the transparent 1:16 planar expansion by laser Doppler velocimetry with a Newtonian liquid and the inelastic, shear thinning fluid P1. Flow at the entry of the smaller channel was straightened with a distributor plate. The model fluids were tested at 25°C in a Rheometrics RFS 8400 rheometer with a cone and plate fixture (5 cm diameter and 0.2 rad. cone angle). The Newtonian fluid was a glycerol/water mixture. The steady shear viscosity curves for two aqueous solutions of hydroxypropyl cellulose ether labeled P1 and P2 are presented in Figure 16; P1 has a power law index of 0.7 above a shear rate of $10\,s^{-1}$ while P2 has a power law index of 0.5. Characteristic relaxation times for P1 and P2 were determined from their dynamic modulus curves presented in Figure 17. Evaluation of the Deborah number confirms that P1 is inelastic under the flow conditions of this study.

Copyright © 2002 John Wiley & Sons, Ltd.

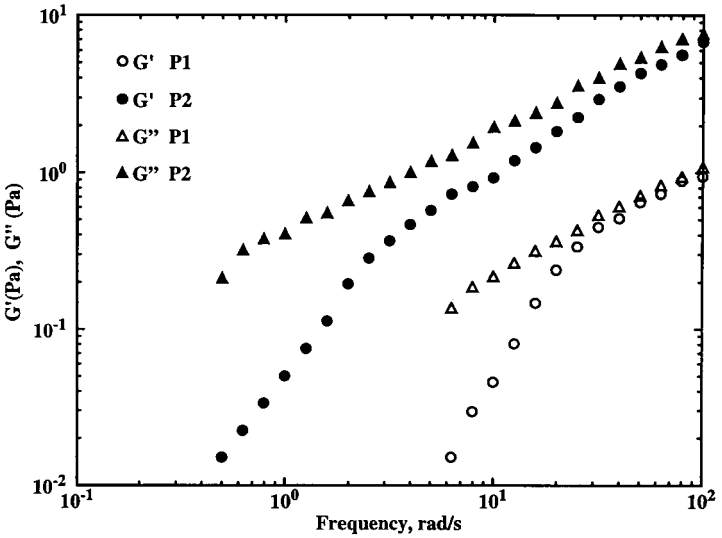

Figure 17. Dynamic moduli for the solutions P1 and P2.

With both fluids, asymmetric flow patterns were observed at Re or $Re^* = 2.5$. This value is considerably lower than the computed onset Reynolds numbers; the lower onset values can be attributed to geometric asymmetry in the experimental apparatus, which arises from the fact that the upstream channel gap dimension could be controlled only to within 5 per cent. The experimental onset value for the P1 solution ($Re_c^* = 1.8$) is greater than that for the Newtonian fluid ($Re_c = 0.8$) like the computed values but the experimental values are closer. The sensitivity to geometric asymmetry is greater for the shear thinning fluid as seen in Figures 8 and 9. Experimentally measured velocity profiles at three axial locations in the downstream channel for the Newtonian liquid and for the shear thinning liquid P1, both at $Re = 2.5$ are presented in Figures 18 and 19 respectively. The second flow transition was so close to the first transition that we present the velocity profiles only after the second transition. Several observations can be made from these figures. The larger corner vortex is clearly smaller with the shear thinning liquid than with the Newtonian liquid. The asymmetric velocity profile is evident very close to the plane of expansion for the Newtonian liquid and farther downstream (at $X = 8$), the profile is clearly asymmetric but the recirculation region is barely perceptible and by $X = 15$, the profile is symmetric. In contrast, the asymmetry becomes prominent farther downstream (at $X = 8$) and is evident to the same extent at $X = 16$ with the shear thinning liquid P1. While the asymmetry persists, there is no recirculating region at $X = 16$ with the shear thinning liquid. Comparison of the velocity profiles for the two liquids at $X = 8$ also reveals that the shear rate at the center of the downstream channel is far greater for the shear thinning fluid. Thus the asymmetry develops more gradually in the case of the shear thinning liquid and the vortex sizes are smaller. While comparing these profiles with those in Figures 12 and 13, we should note that the Reynolds numbers are quite different.

Copyright © 2002 John Wiley & Sons, Ltd.

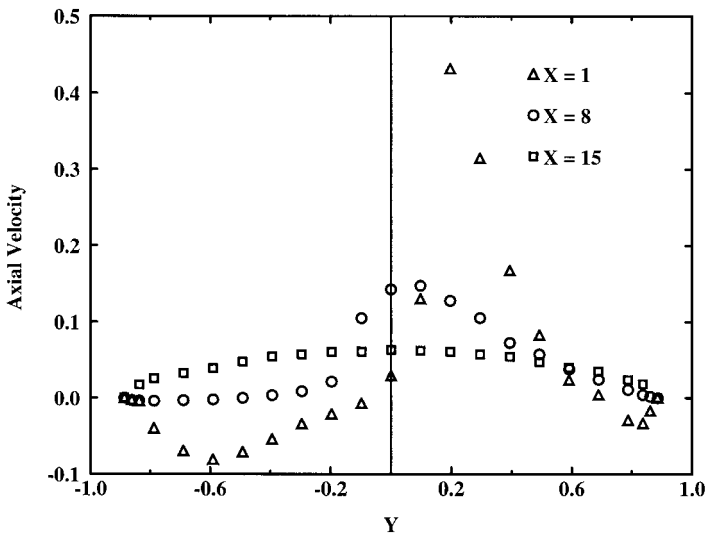

Figure 18. Experimental velocity profiles with a Newtonian model fluid in a 1:16 expansion after the second flow transition at $Re = 2.5$.

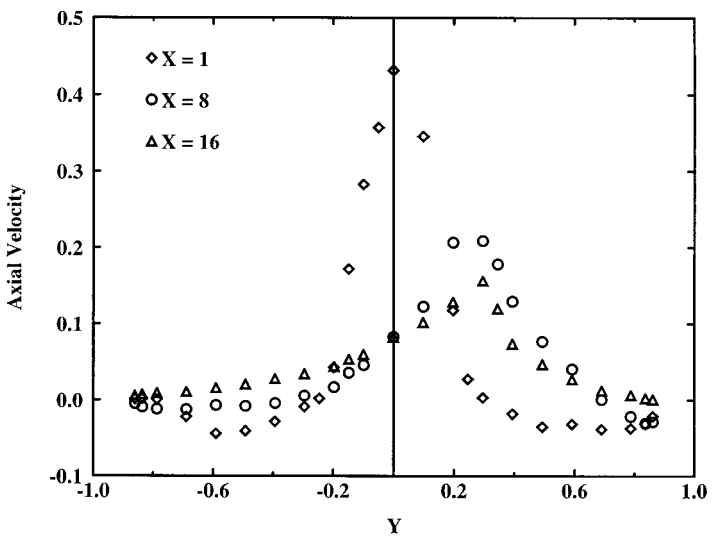

Figure 19. Experimental velocity profiles with the shear thinning liquid P1 in a 1:16 expansion after the second flow transition at $Re^* = 2.5$.

CONCLUSIONS

New results have been obtained with a continuation-domain perturbation method for two successive symmetry breaking flow transitions with increasing Reynolds number in flow of

Copyright © 2002 John Wiley & Sons, Ltd.

generalized Newtonian fluids through a sudden planar expansion with an expansion ratio of 16. The accuracy of this method has been demonstrated by matching results obtained here for a Newtonian fluid through a 1:3 expansion with results in the literature. With an expansion ratio of 16, the onset Reynolds numbers for the two successive flow transitions are found to be close and the onset Reynolds number is particularly sensitive to small geometric perturbations, decreasing with increasing extent of geometric perturbation. After the second transition, the two large staggered vortices on opposite walls occupy most of the transverse dimension so that the core flow between the vortices appears as a thin jet oscillating along the flow direction. As the extent of shear thinning is increased (lower n), the onset Reynolds number is increased; this is consistent with the competing effects of inertia and shear thinning on the vortex size even before the symmetry breaking flow transition. But the degree of asymmetry of the flow decays more slowly along the flow direction with the shear thinning fluid. This feature is also evident in the experimentally observed velocity profiles downstream of the expansion plane for the pseudoplastic fluid. The predicted extent of pressure recovery is lower for shear thinning liquids.

ACKNOWLEDGEMENTS

This research was supported in part by Siemens Automotive Industries, Basell Polyolefins, Michigan Materials and Processing Research Institute and by the State of Michigan Research Excellence Fund through the Composite Materials and Structure Center at Michigan State University.

REFERENCES

1. Cherdron W, Durst F, Whitelaw JH. Asymmetric flows and instabilities in symmetric ducts with sudden expansions. *Journal of Fluid Mechanics* 1978; **84**:13–31.
2. Armaly BF, Durst F, Pereira JCF, Schonung B. Experimental and theoretical investigation of backward-facing step flow. *Journal of Fluid Mechanics* 1983; **127**:473–496.
3. Durst F, Pereira JCF, Tropea C. The plane symmetric sudden-expansion flow at low Reynolds numbers. *Journal of Fluid Mechanics* 1993; **248**:567–581.
4. Alleborn N, Nandakumar K, Raszillier H, Durst F. Further contributions on the two-dimensional flow in a sudden expansion. *Journal of Fluid Mechanics* 1997; **330**:169–188.
5. Fearn RM, Mullin T, Cliffe KA. Nonlinear flow phenomena in a symmetric sudden expansion. *Journal of Fluid Mechanics* 1990; **211**:595–608.
6. Shapira M, Degani D, Weihs D. Stability and existence of multiple solutions for viscous flow in suddenly enlarged channel. *Computers & Fluids* 1990; **18**:239–258.
7. Teschauer I. Numerische Untersuchung der symmetriebrechenden Bifurkation bei Stromungen durch plotzliche Kanalerweiterungen. Studienarbeit Lehrstuhl fur Stromungsmechanik Universitat Erlangen-Nurnberg, 1994.
8. Drikakis D. Bifurcation phenomena in incompressible sudden expansion flows. *Physics of Fluids* 1997; **9**: 76–87.
9. Foumeny EA, Ingham DB, Walker AJ. Bifurcations of incompressible flow through plane symmetric channel flows. *Computers & Fluids* 1996; **25**:225–351.
10. Goodwin RT, Schowalter WR. Interactions of two jets in a channel: solution multiplicity and linear stability. *Journal of Fluid Mechanics* 1996; **313**:55–82.
11. Giaquinta AR, Hung T-K. Slow non-Newtonian flow in a zone of separation. *Journal of the Engineering Mechanics Division—Proceedings of the American Society of Civil Engineers* 1968; **EM6**:1521–1538.
12. Sobey IJ. Observation of waves during oscillatory channel flow. *Journal of Fluid Mechanics* 1985; **151**: 395–426.
13. Sobey IJ, Drazin PG. Bifurcations of two-dimensional channel flows. *Journal of Fluid Mechanics* 1986; **171**: 263–287.

Copyright © 2002 John Wiley & Sons, Ltd.